THE JOURNAL OF
PHYSICAL CHEMISTRY

VOLUME 83, NUMBER 25 DECEMBER 13, 1979

Mechanism of the Photooxidation of Gaseous Formaldehyde

Fu Su, Jack G. Calvert,* and John H. Shaw

Department of Chemistry and Department of Physics, The Ohio State University, Columbus, Ohio 43210 *(Received July 5, 1979)*

Publication costs assisted by the Environmental Protection Agency

Fourier transform infrared spectroscopy has been employed to study the kinetics of product formation in irradiated, dilute (1–100 ppm) CH_2O and CH_2O–Cl_2 mixtures in synthetic air (P_t = 700 torr, 25 °C). The infrared absorbing products of the reaction are identified as HCl, HCO_2H, CO, H_2O_2, and a new metastable product, HO_2CH_2OH. Spectroscopic and kinetic evidence suggest that the new species is formed following HO_2-radical addition to formaldehyde: $HO_2 + CH_2O \rightarrow (HO_2CH_2O) \rightarrow O_2CH_2OH$ (7); $O_2CH_2OH \rightarrow (HO_2CH_2O) \rightarrow HO_2 + CH_2O$ (14); $HO_2 + O_2CH_2OH \rightarrow HO_2CH_2OH + O_2$ (8). The HO_2CH_2OH product decomposes thermally and photochemically to form HCO_2H. In experiments at high [CH_2O], formic acid arises also in a chain reaction following (7): $2O_2CH_2OH \rightarrow 2OCH_2OH + O_2$ (17); $OCH_2OH + O_2 \rightarrow HCO_2H + HO_2$ (18). The following rate constant estimates are derived from the rate data: $k_7 = 1.0 \times 10^{-14}$ cm^3 molecule^{-1} s^{-1}; $k_{14} = 1.5$ s^{-1} (700 torr, 25 °C); $k_{17} = 1.2 \times 10^{-13}$ cm^3 molecule^{-1} s^{-1}.

Introduction

Atmospheric scientists have renewed their interest in the mechanism of formaldehyde photooxidation in recent years[1] in view of the ubiquitous nature of formaldehyde in both the natural and polluted atmospheres and its subsequent role in generation of HO_2 radicals and other products. Recent studies have shown conclusively that two primary processes occur in CH_2O photolysis:[2-8]

$$CH_2O + h\nu \rightarrow H + HCO \quad (I)$$

$$CH_2O + h\nu \rightarrow H_2 + CO \quad (II)$$

The primary process I increases in importance from 3400 Å ($\phi_I \simeq 0.0$) to become the dominant decay path at the shorter wavelengths ($\lambda < 3000$ Å).

Following H-atom and HCO-radical generation in process I in O_2-rich atmospheres the major reactions 1 and 2 are expected to form HO_2 radicals and CO; the extent of peroxyformyl radical generation in reaction 3 remains unclear.[1] Reaction 3 has been considered to be a logical step in a reaction sequence which would lead ultimately to the formic acid product which is observed in Cl_2–CH_2O–O_2 mixture photolyses.[9,10] However, the relative unimportance of CO_2[1] and peroxyformic acid[10,11] product formation in CH_2O photooxidation, and the second-order kinetics of the HCO–O_2 reaction observed in gaseous mixtures up to 1 atm pressure,[12-14] suggest the relative importance of reaction 2 compared to 3 in these systems.

$$H + O_2 + M \rightarrow HO_2 + M \quad (1)$$

$$HCO + O_2 \rightarrow HO_2 + CO \quad (2)$$

$$HCO + O_2 + M \rightarrow HCOO_2 + M \quad (3)$$

Horowitz, Su, and Calvert[1] concluded that reactions involving HO_2 and HO radical addition to CH_2O in addition to reaction 3 could rationalize well the unusual chain processes forming H_2, HCO_2H, and CO products in photolyzed CH_2O–O_2–CO_2 mixtures at 25 °C. In a recent preliminary report,[11] we have presented new spectroscopic evidence that HO_2 radicals add to CH_2O in a sequence of reactions which leads ultimately to formic acid in CH_2O photooxidation at room temperature. We observed a new transient compound, HO_2CH_2OH, which decays to form formic acid. We report here the results of kinetic studies which support this mechanism and further define the reactions and the rate constants which control these interesting new free-radical processes.

* Address correspondence to this author at the Department of Chemistry.

0022-3654/79/2083-3185$01.00/0

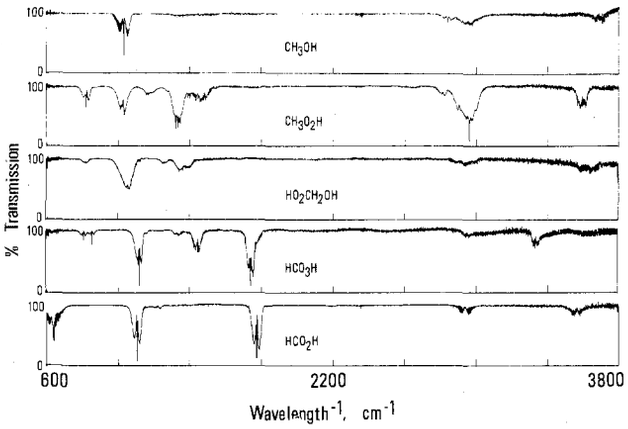

Figure 1. Comparison of the infrared absorption spectra of the new metastable compound (HO_2CH_2OH) and several simple, structurally related compounds.

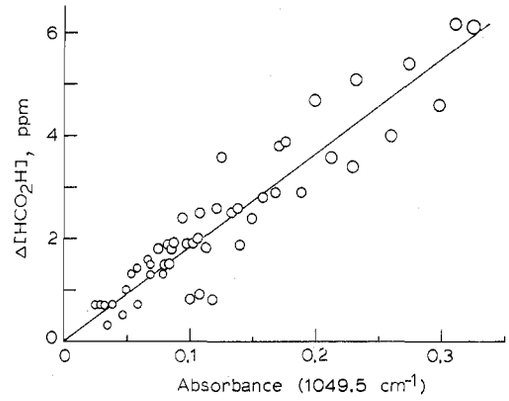

Figure 2. Plot of the absorbance (1049.5 cm^{-1}) of the new compound (HO_2CH_2OH) at the start of the dark period following Cl_2–CH_2O–O_2–N_2 mixture photolyses vs. the increase in the formic acid (ppm) which results during the decay of the new compound in the dark. These data were used to derive the extinction coefficient of the HO_2CH_2OH molecule.

Experimental Section

The FTSIR equipment and photochemical reactor employed in our present experiments have been described previously.[15,16] Photolyses of CH_2O vapor or dilute mixtures of Cl_2 (5–45 ppm) and CH_2O (1–100 ppm) in O_2–N_2 mixtures (P_t = 700 torr, 25 °C) were studied. The wavelength distribution of the ultraviolet lamps which surrounded the large Pyrex reactor mimicked that of sunlight at ground level (z = 40°). The path of the analyzing IR beam was set for 170 m, and the effective resolution of the spectra was 1 cm^{-1}.

The major infrared light absorbing products of the Cl_2–CH_2O–O_2–N_2 mixture photolyses were HCO_2H, HCl, H_2O_2, CO, and a new compound with the unique absorption spectrum shown in Figure 1. It may be compared here to those for several other structurally related simple compounds. The new compound decays slowly in the dark to form HCO_2H, and presumably H_2O, products. In our previous note we have described the spectroscopic evidence which suggests strongly that the new metastable compound is hydroperoxyhydroxymethane (HO_2CH_2OH).[11] The extinction coefficients for the new compound were derived from the results of dark experiments in which the change in absorbance (1049.5 cm^{-1}) of the new compound was correlated with the growth in HCO_2H during the period. See the data in Figure 2. No change in CO or CH_2O occurred as the new compound decayed and the [HCO_2H] grew in these dark experiments. The data of Figure 2 give the extinction coefficient for the new species, ϵ(1049.5 cm^{-1}) = [ln $(I_0/I)/lc$] = 3.3 × 10^{-3} ppm^{-1} m^{-1} for our conditions.

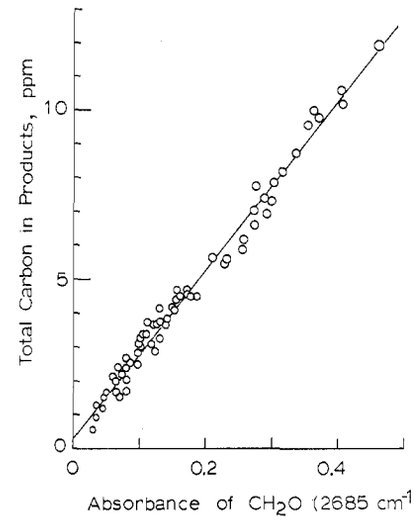

Figure 3. Plot of the total moles of carbon in the products of the Cl_2-sensitized photooxidation of CH_2O vs. the absorbance of CH_2O at 2685 cm^{-1} which leads to these products. These data were used to derive the extinction coefficient for CH_2O vapor.

The extinction coefficients for the infrared bands of all stable products were estimated from Beer's law plots derived from measurements with the pure compounds. In the case of HCO_2H, the measured pressure of formic acid vapor in the gas introduction system was corrected for the presence of the dimer in equilibrium with the monomer.[17] The dimer dissociated nearly completely at the very low concentrations of formic acid achieved after introduction into the large photochemical reactor. Calibration of CH_2O monomer required special attention since it was unstable toward polymerization in the introduction system when introduced at easily measured pressures of pure monomer. In this case very small stable samples (0.5–12 ppm) of monomer were injected into the main reaction cell by passing N_2 gas over the cold, purified liquid monomer. Cl_2 in excess of the CH_2O and O_2 and N_2 were added to a total pressure of 700 torr. The IR spectrum of the initial mixture was determined, and then the Cl_2-photosensitized decomposition of CH_2O was carried out. Following photolysis additional IR spectra were determined to estimate the moles of C-containing products CO and HCO_2H present (following the decay of the metastable HO_2CH_2OH species) as well as the change in CH_2O absorbance at 2685 cm^{-1}. A plot of these data is shown in Figure 3 from which we may estimate the extinction coefficient of CH_2O: ϵ(2685 cm^{-1}) = (2.36 ± 0.08) × 10^{-4} ppm^{-1} m^{-1} for our conditions.

Concentration–time profiles were obtained for all observable compounds in several series of experiments. Typical data are given in Figure 4 for an experiment with initial concentrations of reactants as follows: Cl_2, 15 ppm; CH_2O, 18.9 ppm; O_2, 100 torr; N_2, 600 torr. From such data the rates of product formation and formaldehyde loss could be determined readily for reactions during the early times of the experiment (0–4 min). Three series of rate experiments were made at 700 torr pressure and 25 ± 2 °C. The first two involved Cl_2–CH_2O–O_2–N_2 mixtures and the third used Cl_2-free mixtures of CH_2O–O_2–N_2. In the first series the initial Cl_2 concentration was held essentially constant (5.26 ± 0.03 ppm) while the initial [CH_2O] was varied (101–2.4 ppm). The derived rates from these experiments are summarized in Table I. In the second series the initial [CH_2O] was near constant (~16 ppm), and the initial [Cl_2] was varied (5.3–45 ppm). These data are shown in Table II. In both sets of experiments the O_2 and N_2 (in approximate 1/4 ratio) were in great excess (700 torr total). In the third series of experiments mixtures of pure CH_2O

TABLE I: Rate Data from the Photolyses of Cl_2-CH_2O-O_2-N_2 Mixtures at Constant Initial Cl_2 Concentration[a]

$[CH_2O]_0$, ppm	$[CH_2O]_{av}$,[b] ppm	rates, ppm min^{-1}				$R_{HCO_2H}/R_{HO_2CH_2OH}$
		CO	HCO_2H	HO_2CH_2OH	H_2O_2[c]	
101	97.5	0.96 ± 0.06	0.80 ± 0.06	0.095		0.93
76	73	0.89 ± 0.08	0.63 ± 0.03	0.085		0.98
48.7	46	0.79 ± 0.09	0.47 ± 0.02	0.081		0.70
24.8	23	0.75 ± 0.11	0.29 ± 0.02	0.070		0.48
18.4	17.1	0.79 ± 0.09	0.20 ± 0.01	0.062	(0.1)	0.33
17.0	15.3	0.78 ± 0.12	0.20 ± 0.02	0.066		0.34
8.8	7.5	0.71 ± 0.08	0.10 ± 0.004	0.052	(0.15)	0.21
7.7	6.0	0.68 ± 0.10	0.090 ± 0.002	0.052	(0.12)	0.21
4.3	3.1	0.61 ± 0.06	0.047 ± 0.004	0.0305	(0.14)	0.13
2.6	1.9	0.73 ± 0.09	0.023 ± 0.008	0.0106	(0.15)	0.046
2.4	1.6	0.69 ± 0.05	0.020 ± 0.002	0.0106	(0.20)	0.044

[a] Initial Cl_2 concentrations, 5.26 ± 0.03 ppm; P_{N_2} = 560 torr; P_{O_2} = 140 torr; temperature, 25 ± 2 °C. [b] This is the average $[CH_2O]$ during the period of product rate determinations. [c] The H_2O_2 is near the detection limit in these experiments at low $[Cl_2]_0$, and thus the rates for this compound are very approximate.

TABLE II: Rate Data from the Photolyses of Cl_2-CH_2O-O_2-N_2 Mixtures at Constant Initial CH_2O Concentration[a]

$[CH_2O]_0$, ppm	$[CH_2O]_{av}$,[b] ppm	$[Cl_2]_0$, ppm	rates, ppm min^{-1}				$R_{HCO_2H}/R_{HO_2CH_2OH}$
			CO	HCO_2H	HO_2CH_2OH	H_2O_2	
18.4	17.1	5.27	0.79	0.20	0.062	0.14	0.33
26.3	23.1	9.8	1.55	0.54	0.13	0.22	0.43
19.5	16.7	10.0	1.50	0.44	0.13	0.23	0.38
18.9	15.5	15.0	2.08	0.61	0.17	0.36	0.38
19.7	16.2	20.5	2.80	0.71	0.23	0.47	0.34
18.1	13.1	30.0	4.00	0.86	0.37	0.90	0.31
21.6	17.0	30.0	4.00	1.04	0.37	0.85	0.35
19.4	15.8	45.0	5.65	1.36	0.49	1.28	0.33
20.0	16.1	45.0	5.65	1.36	0.49	1.28	0.33

[a] The initial pressures of O_2 and N_2 were 140 and 560 torr, respectively; temperature, 25 ± 2 °C. [b] This is the average $[CH_2O]$ during the period of product rate determinations.

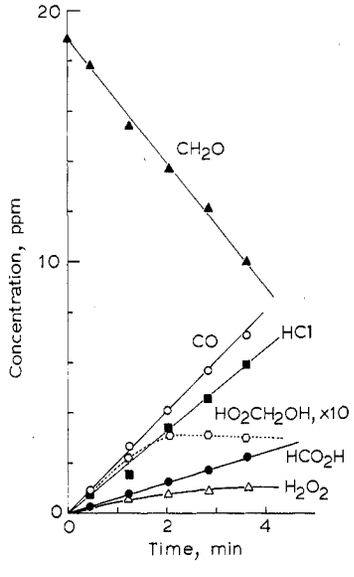

Figure 4. The concentrations of reactants and products as a function of time in the Cl_2-photosensitized oxidation of CH_2O; initial concentrations: Cl_2, 15 ppm; CH_2O, 18.9 ppm; O_2, 100 torr; N_2, 600 torr (25 °C).

(12–104 ppm) in O_2–N_2 mixtures (700 torr total) were photolyzed; rate data from these runs are given in Table III.

Discussion

Mechanism of the Cl_2-Photosensitized Oxidation of Formaldehyde. The spectroscopic identification of the new metastable product of CH_2O photooxidation, HO_2CH_2OH, provides the first direct evidence of HO_2 radical addition to CH_2O.[11] The rate data presented here can be used to define the mechanism and to derive estimates of the rate constants associated with these newly discovered

TABLE III: Rate Data from the Photolyses of CH_2O-O_2-N_2 Mixtures[a]

$[CH_2O]_0$, ppm	rates, ppm min^{-1}		$R_{CO}/[CH_2O]$, min^{-1}
	CO	HCO_2H	
103.5	0.206	0.058	1.99×10^{-3}
67.1	0.153	0.042	2.28×10^{-3}
56.2	0.103	0.0235	1.83×10^{-3}
36.0	0.064	0.0118	1.78×10^{-3}
31.9	0.064	0.0105	2.01×10^{-3}
28.1	0.047	0.0068	1.67×10^{-3}
20.6	0.047	0.0052	2.28×10^{-3}
20.2	0.035	0.0027	1.73×10^{-3}
12.2	0.022	0.0017	1.80×10^{-3}

[a] Initial pressures of O_2 and N_2 are 140 and 560 torr, respectively; temperature, 25 ± 2 °C; the infrared absorptions due to HO_2CH_2OH are observable in these experiments, but because of the very small peaks rate estimates for this compound are very approximate; in the experiment with $[CH_2O]_0$ = 103.5 ppm, $[HO_2CH_2OH] \simeq 0.013 \pm 0.005$ ppm at 3.85 min; in the experiment with $[CH_2O]_0$ = 56.2 ppm, $[HO_2CH_2OH] \simeq 0.009 \pm 0.004$ ppm at 4.55 min.

reactions. The initial rates of formation of the major carbon-containing products of the photolysis of Cl_2–CH_2O–O_2–N_2 mixtures are plotted in Figures 5 and 6. Note in Figure 5 from experiments at constant initial $[Cl_2]$ that the rate of CO formation (corrected for the small rate of CO from direct CH_2O photolysis) is independent of the $[CH_2O]$ over the range 1.6–100 ppm. This behavior is anticipated if CO is derived in the following simple sequence of reactions, where its rate is limited by the Cl_2 photolysis rate, $R_{CO} = R_{HCl} = [Cl_2]2k_4$:

$$Cl_2 + h\nu \rightarrow 2Cl \quad (4)$$

$$Cl + CH_2O \rightarrow HCl + HCO \quad (5)$$

$$HCO + O_2 \rightarrow HO_2 + CO \quad (2)$$

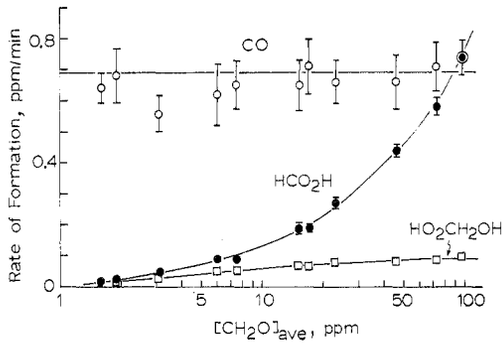

Figure 5. Plot of rates of CO, HCO_2H, and HO_2CH_2OH formation vs. the average $[CH_2O]$ from the Cl_2-photosensitized oxidation of CH_2O; initial $[Cl_2]$ = 5.25 ppm; P_{N_2} = 560 torr; P_{O_2} = 140 torr; solid lines represent the theoretical variation of rates calculated by using the computer simulation of the system employing the mechanism of Table IV.

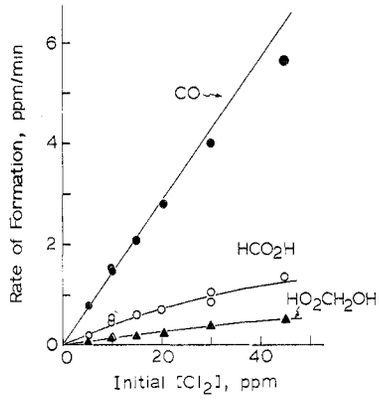

Figure 6. Plot of the rates of CO, HCO_2H, and HO_2CH_2OH formation vs. the initial $[Cl_2]$ from Cl_2-photosensitized oxidation of CH_2O; initial $[CH_2O] \simeq 20$ ppm; P_{O_2} = 140 torr; P_{N_2} = 560 torr; the solid lines represent the theoretical variation of the rates calculated by computer simulation of the system employing the mechanism summarized in Table IV.

In accord with this suggestion is the ratio of the rates of CO and HCl derived from all of the experiments: $R_{CO}/R_{HCl} = 1.1 \pm 0.2$ (2σ). Also the Cl_2 photolysis rate constant obtained from photolyses of Cl_2 (ppm)–H_2 (~10 torr)–O_2–N_2 (690 torr) mixtures, where $R_{HCl} = 2R_{H_2O_2} = 2k_4[Cl_2]$, gave the same values of k_4 as estimated from the Cl_2–CH_2O–O_2–N_2 mixture photolyses within the experimental error. Obviously there is no chain reaction generating CO for these conditions. Note in Figure 6 that R_{CO} is directly proportional to the initial $[Cl_2]$ as is also required by this simple mechanism for CO production.

The present results demand that reaction 2 rather than 3 be the dominant channel for HCO reaction with O_2, even for these experiments in which a total pressure of 700 torr of added air was used. Thus the ratio of CO_2 to CO product for our conditions was less than 0.01, and peroxyformic acid was not observed as a product. The reasonable stability of authentic samples of $HCOO_2H$ in our system would have allowed its detection if it had formed significantly in the Cl_2–CH_2O–O_2–N_2 mixtures. These results coupled with the observed second-order character of the HCO–O_2 reaction up to high added gas pressures[12-14] suggest that reaction 3 is probably not important here.

The HO_2 radicals formed in reaction 2 are expected to react at least in part by reaction 6 to form H_2O_2. The

$$2HO_2 \rightarrow H_2O_2 + O_2 \quad (6)$$

alternative source of H_2O_2 through the possible reaction, $HO_2 + CH_2O \rightarrow H_2O_2 + HCO$, cannot be important here since its occurrence coupled with reaction 2 would lead to

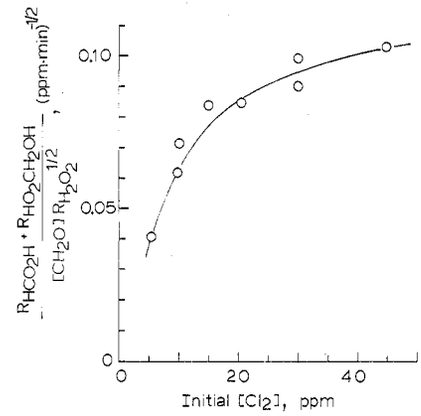

Figure 7. Plot of the rate function 13 of the text vs. the initial $[Cl_2]$; evidence for the reversible nature of the HO_2–CH_2O addition reaction; see the text.

a chain process yielding H_2O_2 and CO which is not observed. However, there is good evidence that HO_2 radicals do react in some way with CH_2O in this system. If only reactions 4, 5, 2, and 6 occurred, we expect $R_{CO}/R_{H_2O_2} = 2$. It can be seen from the data in Figure 4 and Tables I and II that this rate ratio is much greater than 2. This fact and the nature of the new product observed here, HO_2CH_2OH, point to the nature of the additional HO_2 reactions. We suggest that the new product arises following HO_2-radical addition to CH_2O in reaction 7, fol-

$$HO_2 + CH_2O \rightarrow (HO_2CH_2O) \rightarrow O_2CH_2OH \quad (7)$$

$$HO_2 + O_2CH_2OH \rightarrow HO_2CH_2OH + O_2 \quad (8)$$

lowed by reaction 8. The HO_2CH_2OH product which we observe spectroscopically in this system was first suggested by Horner et al.[18] from indirect evidence derived from the high temperature photooxidation of CH_2O over 25 years ago. They postulated that it might be formed in their experiments through the reactions 9 and 10. The H-atom

$$HO_2 + CH_2O \rightarrow HO_2CH_2O \quad (9)$$

$$HO_2CH_2O + CH_2O \rightarrow HO_2CH_2OH + HCO \quad (10)$$

abstraction reaction 10 cannot be important for our system since this would lead to a chain reaction forming HO_2CH_2OH and CO which is not observed. For our conditions it seems likely to us that the initial $HO_2CH_2O\cdot$ radical formed in reaction 7 or 9 will rearrange rapidly by H transfer in a unimolecular reaction involving a five-member ring intermediate to generate the thermodynamically more stable radical species, $\cdot OOCH_2OH$. This radical, like HO_2, is expected to have a significant activation barrier to abstract H atoms from CH_2O, but it could react with HO_2 to form the observed product in reaction 8. This mechanism is also in accord with the observed formation of HO_2CD_2OH from the HO_2 addition to CD_2O.[11]

We observe that HO_2CH_2OH decays in the dark, and more rapidly in the light, to give formic acid, presumably through the reactions 11 and 12. Analogous decay reac-

$$HO_2CH_2OH \text{ (+ wall)} \rightarrow HCO_2H + H_2O \text{ (+ wall)} \quad (11)$$

$$HO_2CH_2OH + h\nu \rightarrow HCO_2H + H_2O \quad (12)$$

tions are observed in our system under similar conditions with two more common peroxy compounds: CH_3OOH ($CH_3OOH \rightarrow CH_2O + H_2O$) and $HCOO_2H$ ($HCOO_2H \rightarrow CO_2 + H_2O$).

If the reactions 4, 5, 2, 6, 7, 8, 11, and 12 alone were responsible for the products observed here, then we would expect the rate expression 13 to hold. This function has

$$(R_{HCO_2H} + R_{HO_2CH_2OH})/[CH_2O]R_{H_2O_2}^{1/2} = k_7/k_6^{1/2} \quad (13)$$

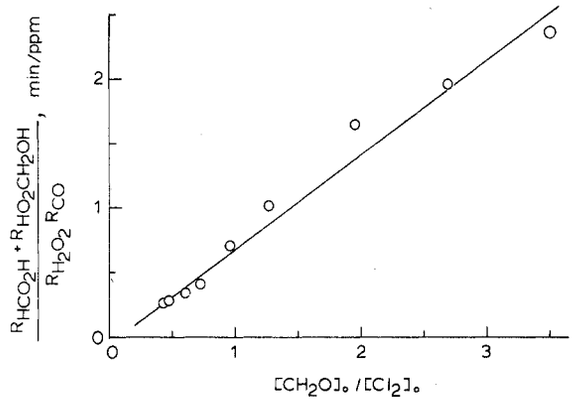

Figure 8. Plot of the function 15 of the text vs. $[CH_2O]/[Cl_2]$; the slope is in theory related to $k_7k_8/[k_{14}k_6(2k_4)]$.

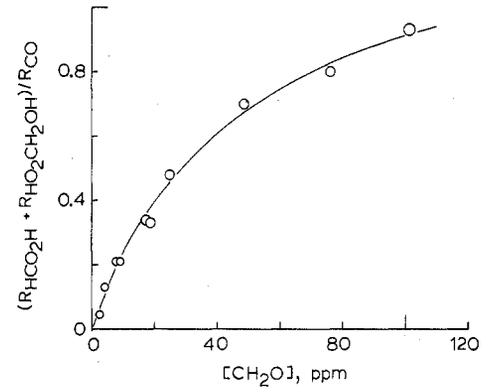

Figure 9. Plot of the ratio of product rates, $(R_{HCO_2H} + R_{HO_2CH_2OH})/R_{CO}$, vs. initial $[CH_2O]$; data from Table I.

been calculated from the rate data of Table II and is plotted vs. initial $[Cl_2]$ in Figure 7. Obviously the function 13 is not independent of $[Cl_2]$ as the mechanism outlined suggests; it shows an increase with increasing $[Cl_2]$. A possible origin of this effect could be the significant occurrence of the reverse of reaction 7 with re-formation of CH_2O and HO_2:

$$O_2CH_2OH \rightarrow (HO_2CH_2O) \rightarrow HO_2 + CH_2O \quad (14)$$

If reaction 14 as well as 7 occurs then in theory the fraction of O_2CH_2OH radicals formed in (7) which ultimately lead to HO_2CH_2OH product in (8) should increase with increasing $[HO_2]$ in the experiments at high $[Cl_2]$. Thus the apparent rate of HO_2 addition to CH_2O would be increased with $[Cl_2]$ increase as we observe in the plot of Figure 7. We may test this hypothesis by considering reaction 14 together with reactions 4, 5, 2, 6, 7, 8, 11, and 12 to rationalize product formation in these experiments. As a first approximation let us assume that the equilibrium, $HO_2 + CH_2O \rightleftharpoons O_2CH_2OH$, is established. Then relation 15 should apply. The rate data from the experiments at high

$$\frac{R_{HCO_2H} + R_{HO_2CH_2OH}}{R_{H_2O_2}R_{CO}} = \frac{[CH_2O]k_7k_8}{[Cl_2]k_{14}k_6(2k_4)} \quad (15)$$

$[Cl_2]$ in Table II, where $R_{H_2O_2}$ values are most reliable, provide the best test of this function. A plot of function 15 vs. $[CH_2O]/[Cl_2]$ ratio is shown in Figure 8. The near linear relationship observed between the variables is consistent with the reaction scheme, including the reversibility of the HO_2 addition step. The slope of the line in Figure 8 gives the estimate $[(k_7k_8/k_{14}k_6(2k_4)] = 0.73 \pm 0.08$ min ppm^{-1}. Taking our experimental estimate for $k_4 = 0.075$ min^{-1}, the literature value for $k_6 = 5.3 \times 10^3$ ppm^{-1} min^{-1},[19] and a reasonable estimate for $k_8 = 3.0 \times 10^3$ ppm^{-1} min^{-1}, the data give $k_7/k_{14} = 0.19 \pm 0.02$ ppm^{-1}. We may also estimate a lower limit for the rate constant for reaction 7 from the value of the ordinate of the plot given in Figure 7 at high $[Cl_2]$ and the experimental value for k_6: $k_7 \geq 10$ ppm^{-1} min^{-1}. We will refine this estimate by using a computer simulation of all of the data after further considerations and additions to the mechanism.

A further test for the compatibility between the rate data and the mechanism outlined can be made from the rate ratios, $(R_{HCO_2H} + R_{HO_2CH_2OH})/R_{CO}$. An HO_2 mass balance based upon the mechanism requires relation 16

$$(R_{HCO_2H} + R_{HO_2CH_2OH})/R_{CO} = 0.5 - (R_{H_2O_2}/R_{CO}) \quad (16)$$

to hold. In our experiments at high $[CH_2O]$ in Table I, where $R_{H_2O_2} \rightarrow 0$, we expect the $(R_{HCO_2H} + R_{HO_2CH_2OH})/R_{CO}$ ratio to maximize near a value of 0.5. We have plotted this ratio vs. $[CH_2O]$ in Figure 9. Obviously this expectation is not realized; the ratio rises above 0.5 in experiments with $[CH_2O] \geq 28$ ppm and continues to climb without maximizing over the range of $[CH_2O]$ studied. Further evidence of the incompleteness of the reaction mechanism is seen in the product ratio, $R_{HCO_2H}/R_{HO_2CH_2OH}$. If HO_2CH_2OH is the only source of HCO_2H in this system as our incomplete mechanism demands, then one expects the ratio to be essentially a constant with variation in initial values of $[CH_2O]$ and $[Cl_2]$. Although this is the case for experiments at constant $[CH_2O]$ in Table II, the ratio is seen to increase strongly with $[CH_2O]$ increase in experiments at constant $[Cl_2]$ in Table I. All of these observations suggest that there is an additional reaction forming formic acid which becomes important at high $[CH_2O]$, and our mechanism is not complete for these conditions. Some clues as to the mechanism of this additional reaction sequence can be had considering the nature of the radicals present at high $[CH_2O]$. In terms of the mechanism outlined we anticipate that the ratio of the concentrations of the two dominant radicals in this system, $[O_2CH_2OH]/[HO_2]$, will increase as the $[CH_2O]$ is raised as a result of the reversible reaction sequence, $HO_2 + CH_2O \rightleftharpoons O_2CH_2OH$. If equilibrium were achieved in these systems the present rate data suggest that the $[O_2CH_2OH]/[HO_2]$ ratio would increase from 0.19 at $[CH_2O] = 1$ ppm to 19 at $[CH_2O] = 100$ ppm. Thus one expects to find the dominance of HO_2 at low $[CH_2O]$ while the O_2CH_2OH radical will be favored at high $[CH_2O]$; in this latter case the O_2CH_2OH–HO_2 interactions required to form HO_2CH_2OH in reaction 8 are much less likely than O_2CH_2OH–O_2CH_2OH interactions. Indeed it is probable that the O_2CH_2OH radicals will react with one another for these conditions in a fashion analogous to that observed with alkyl peroxy radicals ($2RO_2 \rightarrow 2RO + O_2$):

$$2O_2CH_2OH \rightarrow 2OCH_2OH + O_2 \quad (17)$$

In our O_2-rich system the OCH_2OH radical product of (17) should react primarily with O_2 in a fashion analogous to the well-established reaction of the CH_3O radical:

$$OCH_2OH + O_2 \rightarrow HCO_2H + HO_2 \quad (18)$$

Note that reactions 7, 17, and 18 form the elements of a chain process leading to formic acid without generating CO as we observe experimentally.

The rate data from Tables I and II are consistent with the complete mechanism outlined here and summarized in Table IV. The match of the observed product rates with the computer simulations seen in Figures 5 and 6 (solid lines) provides the basis for our best rate constant choices for reactions 7, 14, and 17; published measurements

TABLE IV: Summary of the Mechanism and Rate Constants for the Present Study of the Photolyses of Cl_2-CH_2O-O_2-N_2 Mixtures at 25 °C

no.	reaction	rate constant[a]
4	$Cl_2 + h\nu \rightarrow 2Cl$	1.25×10^{-3}
I	$CH_2O + h\nu \rightarrow H + HCO$	4.2×10^{-6}
II	$CH_2O + h\nu \rightarrow H_2 + CO$	2.8×10^{-5}
1	$H + O_2 + M \rightarrow HO_2 + M$	5.5×10^{-32}
5	$Cl + CH_2O \rightarrow HCl + HCO$	7.4×10^{-11}
2	$HCO + O_2 \rightarrow HO_2 + CO$	5.6×10^{-12}
6	$HO_2 + HO_2 \rightarrow H_2O_2 + O_2$	3.6×10^{-12}
7	$HO_2 + CH_2O \rightarrow (HO_2CH_2O) \rightarrow O_2CH_2OH$	1.0×10^{-14}
8	$HO_2 + O_2CH_2OH \rightarrow HO_2CH_2OH + O_2$	2.0×10^{-12}
12	$HO_2CH_2OH + h\nu \rightarrow HCO_2H + H_2O$	3.9×10^{-2}
11	HO_2CH_2OH (+ wall) $\rightarrow HCO_2H + H_2O$ (+ wall)	2.8×10^{-3}
14	$O_2CH_2OH \rightarrow (HO_2CH_2O) \rightarrow HO_2 + CH_2O$	1.5
17	$2O_2CH_2OH \rightarrow 2OCH_2OH + O_2$	1.2×10^{-13}
18	$OCH_2OH + O_2 \rightarrow HCO_2H + HO_2$	6.1×10^{-16}

[a] Rate constants are in units of cm^3 molecule^{-1}/s^{-1} except for reactions I, II, 4, 11, and 12 which are s^{-1} and reaction 1 which is cm^2 molecule^{-2}/s^{-1}; see the text for the reasoning, references, and methods of measurement employed; rate constants refer to the condition of total pressure (N_2, O_2) equal 700 torr at 25 °C.

were used for the rate constants of reactions 1,[19] 2,[12-14] 5,[20] and 6.[19] We used estimates of the rate constants for (8) and (18) which are consistent with those measured for the analogous reactions between HO_2–HO_2 and CH_3O–O_2, respectively.

We may check on the consistency of the present experimental estimates of the rate constants k_7 and k_{14} by using thermochemical methods.

$$HO_2 + CH_2O \rightleftharpoons O_2CH_2OH \qquad (7,14)$$

From Benson's additivity rules we can estimate that $\Delta H_7° \simeq -16.8$ kcal/mol and $\Delta S_7° \simeq -32.7$ eu (25 °C, 1 atm standard state).[21] From these we calculate $k_7/k_{14} = e^{-\Delta H°/RT} e^{\Delta S°/R} \simeq 1.5 \times 10^5$ atm^{-1} = 0.15 ppm^{-1} (25 °C). This checks well with the ratio of the experimental kinetic estimates of the individual constants: $k_7/k_{14} = 0.17$ ppm^{-1}. The mechanism appears to be self-consistent and can rationalize all of the data which we have obtained in this work.

Photooxidation of Formaldehyde Vapor in N_2–O_2 Mixtures. The mechanism outlined above may be applied to the rate data of the Cl_2-free system summarized in Table III. The rate of HO_2 generation from CH_2O photodecomposition in process I is very much lower than the rate of HO_2 generation from Cl_2 photolyses in CH_2O–Cl_2 mixtures. As a result the H_2O_2 and HO_2CH_2OH are minor products for these conditions. Note in Table III that the ratio of $R_{CO}/[CH_2O]$ is essentially a constant with variation in $[CH_2O]$ from 104 to 12 ppm; since there is no chain process forming CO in this system, the average value of this ratio gives our best experimental estimate of $k_I + k_{II} = (1.93 \pm 0.15) \times 10^{-3}$ min^{-1} = $(3.2 \pm 0.2) \times 10^{-5}$ s^{-1}. The ratio of k_I/k_{II} was obtained from a computer match of the product data by using the complete reaction mechanism of Table IV. The best fit of the CO, HCO_2H, and HO_2CH_2OH product rate data shown in Figure 10 gave $k_I = 4.2 \times 10^{-6}$ and $k_{II} = 2.8 \times 10^{-5}$ s^{-1} for our conditions. These experimental values are in accord with theoretical estimates calculated by using the experimentally measured wavelength distribution of the light within the cell,[15,16] the variation of ϕ_I, ϕ_{II}, and ϵ for CH_2O with wavelength,[2,6] our experimental value for k_4 in the cell, and Cl_2 extinction data.

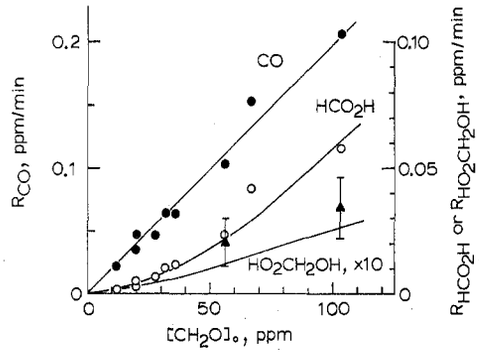

Figure 10. Plot of the rates of CO, HCO_2H, and HO_2CH_2OH products vs. initial $[CH_2O]$ from the photolyses of CH_2O–O_2–N_2 mixtures; the solid lines are the theoretical variation of rates predicted from the computer simulation of the system by using the mechanism summarized in Table IV.

The kinetic data derived here may be used to predict the significance of the HO_2CH_2OH transient species in the polluted atmosphere. The rate of HO_2CH_2OH formation (ppm min^{-1}) should be given approximately by the function, $R_{HO_2CH_2OH} \simeq [HO_2]^2[CH_2O]k_8k_7/k_{14} = [HO_2]^2 \cdot [CH_2O](5.0 \times 10^2)$. For typical reactant concentrations expected within the hydrocarbon–NO–NO_2-polluted, sunlight-irradiated troposphere ($[CH_2O] = 0.02$ ppm, $[HO_2] = 2 \times 10^{-4}$ ppm), $R_{HO_2CH_2OH} \simeq 0.4$ ppt min^{-1}. Whether this rate is sufficient to generate levels of the transient which are detectable will depend upon the loss rate of this species in air. If the photolysis in the lower atmosphere is as fast as our cell data suggest, then the steady state level of HO_2CH_2OH will reach only about 0.2 ppt in a highly polluted lower atmosphere.

Attempts to correlate human eye irritation in smog chambers with specific products have pointed to possible associations with the concentrations of CH_2O, acrolein, peroxyacetyl nitrate, and possibly other reactive species in the atmosphere.[22-24] It is possible that the presumed influence of CH_2O on eye irritation might lie in its direct relation to the rates of generation of HO_2CH_2OH and HCO_2H products which create a much greater irritation than CH_2O itself.

Acknowledgment. This work was supported by a research grant from the Environmental Protection Agency (R-806479-01-0). We are grateful to Dr. Hiromi Niki for helpful discussions related to the mechanism of the Cl_2-photosensitized oxidation of CH_2O.

References and Notes

(1) A. Horowitz, F. Su, and J. G. Calvert, *Int. J. Chem. Kinet.*, **10**, 1099 (1978); references to the earlier work are given here.
(2) A. Horowitz and J. G. Calvert, *Int. J. Chem. Kinet.*, **10**, 805 (1978).
(3) R. S. Lewis, K. Y. Tang, and E. K. C. Lee, *J. Chem. Phys.*, **65**, 2910 (1976).
(4) J. Marling, *J. Chem. Phys.*, **66**, 4200 (1977).
(5) J. H. Clark, C. B. Moore, and N. S. Nogar, *J. Chem. Phys.*, **68**, 1264 (1978).
(6) G. K. Moortgat, F. Slemr, W. Seiler, and P. Warneck, *Chem. Phys. Lett.*, **54**, 444 (1978).
(7) R. S. Lewis and E. K. C. Lee, *J. Phys. Chem.*, **82**, 249 (1978).
(8) K. Y. Tang, P. W. Fairchild, and E. K. C. Lee, *J. Phys. Chem.*, **83**, 569 (1979).
(9) T. L. Osif and J. Heicklen, *J. Phys. Chem.*, **80**, 1526 (1976).
(10) H. Niki, P. Maker, C. Savage, and L. Breitenbach, Abstracts of the 173rd National Meeting of the American Chemical Society, New Orleans, La., March 20–25, 1977.
(11) F. Su, J. G. Calvert, J. H. Shaw, H. Niki, P. D. Maker, C. M. Savage, and L. P. Breitenbach, *Chem. Phys. Lett.*, **65**, 221 (1979).
(12) N. Washida, R. I. Martinez and K. D. Bayes, *Z. Naturforsch. A*, **29**, 251 (1974).

(13) J. P. Reilly, J. H. Clark, C. B. Moore, and G. C. Pimentel, *J. Chem. Phys.*, **69**, 4381 (1978).
(14) K. Shibuya, T. Ebata, K. Obi, and I. Tanaka, *J. Phys. Chem.*, **81**, 2292 (1977).
(15) F. Su, J. G. Calvert, C. R. Lindley, W. M. Uselman, and J. H. Shaw, *J. Phys. Chem.*, **83**, 912 (1979).
(16) W. M. Uselman, S. Z. Levine, W. H. Chan, J. G. Calvert, and J. H. Shaw, "Nitrogenous Air Pollutants", D. Grosjean, Ed., Ann Arbor Science, Ann Arbor, Mich., 1979, Chapter 2, p 17.
(17) J. Chao and B. J. Zwolinski, *J. Phys. Chem. Ref. Data*, **7**, 363 (1978).
(18) E. C. A. Horner, D. W. G. Style, and D. Summers, *Trans. Faraday Soc.*, **50**, 1201 (1954).
(19) R. F. Hampton, Jr., and D. Garvin, *Natl. Bur. Stand., Spec. Publ.*, **No. 513** (1978).
(20) H. Niki, P. D. Maker, L. P. Breitenbach, and C. M. Savage, *Chem. Phys. Lett.*, **57**, 596 (1978); J. V. Michael, D. S. Nava, W. A. Payne, and L. J. Stief, *J. Chem. Phys.*, **70**, 1147 (1979).
(21) S. W. Benson, "Thermochemical Kinetics", 2nd ed, Wiley, New York, 1976.
(22) J. M. Heuss and W. A. Glasson, *Environ. Sci. Technol.*, **2**, 1109 (1968).
(23) W. E. Wilson, Jr., A. Levy, and E. H. McDonald, *Environ. Sci. Technol.*, **6**, 423 (1972).
(24) A. P. Altshuller, *J. Air Pollut. Control Assoc.*, **28**, 594 (1978).

Flash Photolysis–Resonance Fluorescence Kinetics Study of the Reaction OH + NO_2 + M → HNO_3 + M

P. H. Wine,* N. M. Kreutter, and A. R. Ravishankara*

Molecular Sciences Group, Engineering Experiment Station, Georgia Institute of Technology, Atlanta, Georgia 30332

(Received July 18, 1979)

Publication costs assisted by the National Science Foundation

The flash photolysis–resonance fluorescence technique has been employed to study the kinetics of the combination reaction OH + NO_2 + M → HNO_3 + M. A total of 57 bimolecular rate constants are reported for varying conditions of temperature (247–352 K), pressure (14–700 torr), and diluent gas identity (He, Ar, N_2, SF_6). These new rate data are compared with previous measurements, and their significance to atmospheric chemistry and unimolecular rate theory is discussed.

Introduction

The kinetics of the reaction

$$OH + NO_2 + M \rightarrow HNO_3 + M \qquad (1)$$

has been the subject of extensive investigation in recent years. This interest has been stimulated by the importance of reaction 1 as a sink for reactive HO_x and NO_x species in the atmosphere. Also, because reaction 1 is in the "fall-off" region between third- and second-order kinetics over the range of total pressures typically accessible to laboratory studies, it is of considerable interest as a test for theories of unimolecular decomposition–recombination reaction rates.[2-4]

Most direct measurements of k_1 have been carried out in discharge-flow systems at total pressures of less than 10 torr.[5-12] Measurements at higher pressures have been reported by Smith and co-workers[13-15] using the flash photolysis–resonance absorption technique and by Atkinson et al.[16] using the flash photolysis–resonance fluorescence technique. Because N_2 quenches electronically excited OH very efficiently, the flash photolysis–resonance fluorescence study could not obtain data under conditions which are directly applicable to atmospheric chemistry. Therefore, the choice of k_1 for input into atmospheric models relies heavily on results from a single laboratory.[13-15] The present study was undertaken to reduce the uncertainty in k_1 under atmospheric conditions and also to broaden the available data base for testing unimolecular reaction rate theories. Bimolecular rate constants are reported for a wide range of temperatures (247–352 K), pressures (14–700 torr), and diluent gases (He, Ar, N_2, SF_6). Of particular interest is the fact that measurements have been carried out using resonance fluorescence detection of OH at nitrogen pressures up to 225 torr. The improvements in OH detection sensitivity which allowed these measurements to be made are discussed.

Experimental Section

The apparatus used in this study has been described previously.[17,18] Hence, we will describe the system briefly and elaborate only on new modifications.

An all-Pyrex jacketed reaction cell with an internal volume of ~150 cm^3 was used in all experiments. The cell was maintained at a known constant temperature by circulating either methanol (247–297 K) or ethylene glycol (297–352 K) from a thermostated bath through the outer jacket. OH radicals were produced by the flash photolysis of H_2O at wavelengths between the onset of absorption at 185 nm and the Suprasil cutoff at ~165 nm. An OH resonance lamp situated perpendicular to the flash lamp excited resonance fluorescence in the 0–0 band of the $A^2\Sigma^+ - X^2\pi$ system; this fluorescence was detected perpendicular to both the flash lamp and resonance lamp by a photomultiplier fitted with an interference filter (3095-Å peak transmission, 100-Å FWHM). Signals were obtained by photon counting and then fed into a signal averager operating in the multichannel scaling mode. For each decay rate measured, sufficient flashes were averaged to obtain a well-defined temporal profile over at least three $1/e$ times.

In order to avoid the accumulation of photolysis or reaction products, all experiments were carried out under "slow-flow" conditions.[18] NO_2 was flowed from a 12-L bulb containing a dilute NO_2/diluent mixture; in all cases, the fraction of NO_2 which existed as N_2O_4 in the storage bulb was negligible. The water mixture was generated by bubbling diluent gas through distilled water at room temperature and a pressure of 800 torr. The NO_2 mixture, water mixture, and additional diluent gas were premixed before entering the reaction cell. Concentrations of each component in the reaction mixture were determined from measurements of the appropriate mass flow rates and the total pressure. The fraction of NO_2 in the NO_2/diluent mixture was checked frequently by simultaneous mea-

0022-3654/79/2083-3191$01.00/0